Nonlinear Analysis: Modelling and Control, Vol. 31, No. 2, 443–462
https://doi.org/10.15388/namc.2026.31.45383

Vilnius University Press

Entropy generation for MHD pulsating stratified liquid flow between two permeable beds

Madhurya Vangalapudi[1], **Suripeddi Srinivas**

VIT-AP University, Amaravathi, AP, India
madhurya6699@gmail.com; srinusuripeddi@hotmail.com

Received: April 1, 2025 / **Revised:** December 6, 2025 / **Published online:** February 16, 2026

Abstract. In natural systems such as lakes, reservoirs, and the upper ocean layers, temperature-induced stratified fluid flows are frequently observed. Numerous studies have explored key aspects of these flows, including stability, mixing, and thermal transport. However, the heat transfer characteristics of stratified fluid flow between permeable beds remain unexplored. This study aims to address this gap by performing an entropy generation analysis of pulsating stratified fluid flow between two permeable beds, with key applications in geothermal energy extraction, environmental modelling, and biomedical engineering. Liquid is injected through the lower bed and extracted from the upper bed at an equal velocity. The governing flow equations are solved numerically using the fourth-order Runge–Kutta (RK-4) method in combination with the shooting method in Mathematica. Graphical results are presented to illustrate the influence of key parameters on velocity, temperature, Nusselt number, entropy generation, Bejan number, mass flux, and stress distribution. Our results indicated that a rise in the Reynolds number, pressure gradient, and stratification parameter boosts the fluid velocity, while a higher slip parameter tends to reduce it. The temperature distribution declines with the rise of magnetic field and Reynolds number. In contrast, it intensifies with elevated Brinkman number, pressure gradient, and stratification parameter.

Keywords: stratified fluid, permeable bed, Bejan number, Nusselt number.

1 Introduction

The flow between permeable beds is crucial in groundwater movement, oil and gas reservoirs, and contaminant transport, impacting resource extraction and environmental sustainability. However, literature on flow dynamics between permeable layers remains limited as documented in references [2, 4, 9, 11, 14, 15, 17, 21, 26, 27, 29, 31]. In view of this, Channabasappa and Ranganna [4] investigated the impact of velocity slip and the viscous stratification factor on flow over a permeable surface. Their study reveals that a rise in slip parameter boosts the mass flow rate, while greater permeability diminishes it. Additionally, viscosity stratification promotes a higher mass flow rate. The influence

[1]The author was financially supported by a research fellowship from VIT-AP University, Amaravathi-522237, India.

of an aligned magnetic field on the flow of a steady, laminar, viscous, incompressible, conducting liquid in an open inclined channel, with the lower boundary formed by a bed of varying permeability and the free surface exposed to atmospheric pressure, has been studied by Jagadeeswara Pillai et al. [21]. Vajravelu et al. [31] examined the pulsatile motion of a viscous liquid confined between permeable beds. Their study explores liquid motion using Navier–Stokes equations between the beds and Darcy's law within them, deriving velocity and volume flux. Malathy and Srinivas [15] studied pulsating MHD flow between two permeable beds with equal injection and suction. Entropy generation in the steady transport of two immiscible couple-stress fluids through a horizontal channel with porous boundaries at the top and bottom was studied by Srinivas et al. [26]. In their study, the couple stresses in the fluid lead to a reduction in both velocity and temperature. As the Darcy number becomes larger, the entropy generation rate near the channel walls lessens, and the Bejan number rises. Srinivas and Ramana Murthy [27] examined the behavior of immiscible couple stress liquids between permeable beds. Their study unveiled that the velocity enhances with rise of Reynolds and Darcy numbers, but it diminishes with the slip parameter. Moreover, reduced permeability in the beds leads to an increase in flow rate. The analysis focuses on the pulsatile flow of a viscous stratified fluid with variable viscosity between permeable beds, which is analysed by Avinash et al. [2]. Their study reveals that a rise in the stratification results in a fall in fluid density and viscosity, consequently enhancing the flow velocity. Deepak and Manju [11] derived the velocity, temperature, mass flux, skin friction, and heat transfer rate expressions by analytically solving the governing equations for MHD pulsating flow and heat transfer in two immiscible, incompressible, and conducting couple-stress liquids confined between porous boundaries. The role of the ion diffusion coefficient in steady electroosmotic couple-stress nanofluid flow and heat transfer within a porous microchannel bounded by permeable beds was explored by Mukharjee and Shit [17]. Recently, a fractal geometry approach to modelling stress-sensitive permeability in porous media with fluid-solid interaction was explored by Tan et al. [29]. Very recently, Madhurya and Srinivas [14] analyzed the flow of immiscible liquid layers exhibiting couple-stress and micropolar effects between permeable beds with entropy generation.

Stratification refers to the formation of fluid layers, such as in water or air, resulting from density variations with height, often driven by differences in temperature or salinity. Understanding stratification is crucial for analyzing fluid stability, internal gravity waves, and mixing processes in natural and engineered systems. In light of these aspects, a wide range of studies have explored pulsatile flow in Stratified fluids under various conditions, as documented in references [1, 13, 18, 22, 23, 32] and other pertinent literature. Long [13] studied the experimental and theoretical aspects of internal fluid oscillations in a gravity field with vertical density and velocity gradients. The behavior of compressible and incompressible inviscid fluids in a stationary multilayer stratified system is analysed using the linearised Euler equations. A key finding is that several characteristics of a multilayer system are universal, meaning they remain independent of factors such as the number of layers, their thicknesses, the fluids' equations of state, and the equilibrium density distributions examined by Yang and Zhang [32]. Ardekani and Stocker [1] analysed fundamental solutions for low Reynolds number flows in a stratified fluid, addressing scenarios

such as a point force and a doublet. Their study reveals that stratification significantly modifies the liquid flow by generating toroidal eddies and causing the velocity to decay more rapidly compared to homogeneous liquid. Prakash et al. [22] examined the impact of thermal characteristics on the magnetohydrodynamic flow of a stratified viscoelastic liquid within a permeable medium within a parallel plate channel positioned at θ. The governing flow equations are solved using a perturbation approach, yielding mathematical expressions for velocity, temperature, Nusselt number, skin friction, and flow flux in the channel for both fluid and particle phases. The study by Xiaohang et al. [23] explored the use of artificial interface oscillations to promote direct contact heat transfer between two stratified immiscible fluids. The flow of melting heat in quadratic stratified Jeffrey liquid near the stagnation point is examined by Mamoona et al. [18]. In their study, flow is influenced by a linearly stretchable sheet, heat transport characteristics are analysed by considering viscous dissipation and heat generation or absorption, a constant magnetic field is applied to the electrically conducting liquid in the vertical direction, and the governing equations are solved using the Homotopy method.

Pulsatile flow enhances heat transfer by inducing periodic fluctuations that promote better mixing and reduce thermal boundary layers. This dynamic flow pattern improves the interaction between the fluid and solid surfaces, boosting thermal conductivity. In heat transfer applications, such as geothermal systems, pulsatile flow leads to more efficient heat extraction and storage. Further, numerous studies have investigated accounting the heat transfer characteristics on pulsatile and peristaltic flows for the cases of both Newtonian and non-Newtonian fluids; see [5, 7, 8, 12, 16, 20, 24, 25, 28, 30] and other relevant literature. Radhakrishnamacharya and Maiti [24] explored the impact of thermal effects on Newtonian viscous flow through a porous zone subjected to an oscillatory pressure gradient. Mandal [16] conducted a theoretical study to investigate key characteristics of nonlinear blood flow through a constricted, flexible artery under the influence of a pulsating pressure gradient. The blood flow was modelled using a two-liquid approach with a core region of erythrocyte suspension treated as a non-Newtonian fluid, and a peripheral plasma layer represented as a Newtonian liquid. Bharatkumar and Srinivas [12] investigated the pulsating flow of an Eyring–Powell nanofluid in a porous channel under the influence of a magnetic field. In their study, blood served as the non-Newtonian base fluid, while gold and aluminium oxide were utilised as nanoparticles. Padma and Srinivas [7] examined the oscillatory flow of two immiscible, viscous liquids under MHD effects in a porous channel with heat transfer. In their analysis, liquid layers with varying viscosities flow through the different regions, and the governing equations for the flow are solved using the regular perturbation technique, which yields analytical expressions for velocity and temperature distribution. Recently, Komal and Srinivas [8] numerical investigated the time-dependent two-layered immiscible flow through a curved corrugated channel under the influence of a magnetic field. Their results revealed that the shear stress decreases with an increase in the frequency parameter but rises with a higher Hartmann number at the outer wall of the channel, whereas the opposite trend is observed at the lower wall.

Direct-contact heat transfer in stratified fluids is frequently encountered in industries such as solar salt production, desalination, and petrochemical engineering. Information

related to time-dependent flows involving thermal effects in stratified fluids is limited, and not much work is reported in the literature. In such flows, entropy generation quantifies the irreversibilities within thermofluid systems, providing insight into energy losses due to heat transfer, viscous dissipation, and other dissipative effects. Motivated by the previous works [2, 4, 17], the present research aims to explore entropy generation analysis for pulsating stratified liquid flow between permeable beds. The flow is subjected to the pulsatile pressure gradient, while accounting for the effects of magnetic field, viscous dissipation, radiative heat flux, and Joule heating. Liquid is injected through the LPB and extracted from the UPB at an equal rate. The Beaver–Joseph slip boundary conditions [3] are used at liquid-permeable bed interfaces. The governing equations are solved numerically using the fourth-order Runge–Kutta method combined with the shooting method in Mathematica. Graphical results are provided to illustrate how key parameters influence velocity, temperature, Nusselt number, entropy generation, Bejan number, mass flux, and stress distribution. The present results show good agreement with Malathy and Srinivas [15] in the limiting case $\beta \to 0$ and with Avinash et al. [2] for the hydrodynamic case.

1.1 Mathematical framework

Figure 1 presents a physical model of the problem consisting of an infinite channel with permeable beds. The x-axis lies along the lower permeable bed interface, while the y-axis is perpendicular. The permeable bed interfaces are at $y = 0$ and $y = h$. The system involves pulsating stratified liquid flow between porous beds. Liquid is injected into the channel from the lower permeable bed (LPB) with a constant velocity V and is extracted from the upper permeable bed (UPB) at the same velocity. The LPB and UPB have permeabilities k_1 and k_2, and their constant temperatures are T_{w1} and T_{w2}, respectively. Flow within the LPB and UPB adheres to Darcy's law [26], while the liquid flow between these layers is dictated by the stratified liquid flow equations. The following assumptions are considered in this analysis: (a) the flow remains laminar and fully developed; (b) the permeable beds are uniform in nature; (c) the fluid is driven by a varying pressure gradient over time; (d) the viscosity and density falls exponentially with respect to y, i.e., $\mu = \mu_0 \mathrm{e}^{-\beta y}$ and $\rho = \rho_0 \mathrm{e}^{-\beta y}$, where $\beta > 0$ is the stratification factor [1,2,4]. Here μ_0 and ρ_0 denote the viscosity and density at $y = 0$.

Darcy's law [6], which states that the filtration velocity of a fluid is directly proportional to the pressure gradient, is a basic principle for explaining flow in porous media with low permeability. It is also the most widely used and simplest model in this field. In 1856, French engineer Henry Darcy carried out experiments to investigate the behavior of water as it flowed downward through a vertical column of homogeneous sand. Through his experiments, he established a proportionality between the water flow rate q and the applied pressure difference ∇P expressed as

$$\bar{q} = -\frac{K}{\mu} \nabla P,$$

where K is the permeability, and μ represents the fluid's dynamic viscosity.

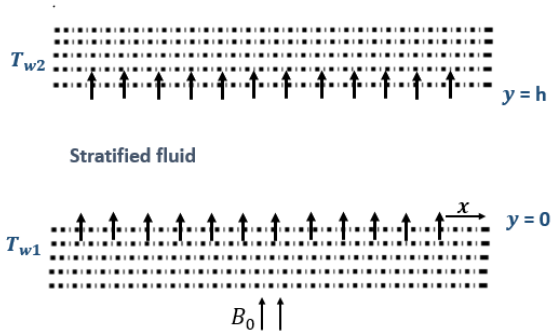

Figure 1. Physical model.

When liquid flows past an impermeable surface, the no-slip condition generally applies at boundary. However, for permeable surfaces, this condition no longer holds due to liquid migration occurring tangentially within the porous medium. In such cases, the no-slip condition becomes invalid as the liquid moves along the boundary inside the porous structure. Through experimental investigations, Beavers and Joseph [3] established that the velocity slip is related to tangential stress, a relationship now recognized as the BJ condition

$$\frac{\mathrm{d}U}{\mathrm{d}Y} = \frac{\alpha}{\sqrt{K}}(U_B - Q),$$

where U_B, Q , K, and α represent the velocity slip, velocity within the porous bed, permeability and slip coefficient, respectively [3, 26, 33]. The value $\alpha = 0$ corresponds to a perfect slip condition, while in the limit $\alpha \to \infty$, the no-slip condition is recovered, implying ($U_B = Q$). Additionally, as $K \to \infty$, the surface behaves as impermeable, resulting in zero normal velocity at the interface [19].

The governing flow equation and boundary conditions [2, 4, 10, 23]:

$$\frac{\partial u}{\partial t} + V\frac{\partial u}{\partial y} = -\frac{1}{\rho}\frac{\partial P}{\partial x} + \frac{1}{\rho}\frac{\partial}{\partial y}\left(\mu\frac{\partial u}{\partial y}\right) - \frac{\sigma {B_0}^2}{\rho}u, \tag{1}$$

$$\frac{\partial T}{\partial t} + V\frac{\partial T}{\partial y} = \frac{k}{\rho C_p}\frac{\partial^2 T}{\partial y^2} + \frac{\upsilon}{C_p}\left(\frac{\partial u}{\partial y}\right)^2 - \frac{1}{\rho C_p}\frac{\partial q_r}{\partial y} + \frac{\sigma {B_0}^2}{\rho C_p}u^2, \tag{2}$$

$$\frac{\partial u}{\partial y} = \frac{\alpha}{\sqrt{K_1}}\left(u_{B1} - Q_1\right) \quad \text{at } y = 0, \tag{3}$$

$$\frac{\partial u}{\partial y} = -\frac{\alpha}{\sqrt{K_2}}\left(u_{B2} - Q_2\right) \quad \text{at } y = h. \tag{4}$$

Nondimensional flow quantities: $x^* = x/h$, $y^* = y/h$, $u_j^* = u_j/V$, $t^* = tV/h$, $p^* = p/(\rho V^2)$, $\theta^* = (T_i - T_{w1})/(T_{w2} - T_{w1})$, $\sigma_1 = h/\sqrt{K_1}$, $\sigma_2 = h/\sqrt{K_2}$, $M = B_0 h\sqrt{\sigma/(\rho_1 \upsilon_1)}$, $R = \rho u h/\mu$, $Pr = \mu Cp/k$, $Br = \mu V^2/(k\Delta T)$, $Rd = 4\sigma' T^3/k^* k$). Here the terms M, σ, Ω, R, Cp, Rd, Pr, σ_i, υ, and Br correspond to the Hartmann number, electrical conductivity, temperature difference, Reynolds number, specific heat,

thermal radiation, Prandtl number, permeability parameter, kinematic coefficient of viscosity, and Brinkman number, respectively, while B_0 denotes the external magnetic field, and the radiative heat flux using the Rosseland approximation is given by $q_r = 4\sigma'/(3k^*)\cdot\partial T^4/\partial y$, $\sigma = 5.6697\cdot 10^{-8}\,\mathrm{W,m^{-2}K^{-4}}$, where σ' is the Stefan–Boltzmann constant, and k^* represents the Rosseland mean absorption coefficient. Assume that only slight temperature variations occur within the liquid [7], and represent T'^4 as a linear function of T': $T'^4 \cong 4T_0^3T' - 3T_0^4$.

After nondimensionalizing and omitting the asterisks, Eqs. (1)–(4) become

$$\frac{\partial u}{\partial t} + V\frac{\partial u}{\partial y} = -\frac{\partial P}{\partial x} + \frac{1}{R}\left(-\beta\frac{\partial u}{\partial y} + \frac{\partial^2 u}{\partial y^2}\right) - \frac{M^2}{R}\mathrm{e}^{\beta y}u,$$

$$\frac{\partial \theta}{\partial t} + V\frac{\partial \theta}{\partial y} = \frac{\mathrm{e}^{\beta y}}{RPr}\frac{\partial^2\theta}{\partial y^2} + \frac{Ec}{R}\left(\frac{\partial u}{\partial y}\right)^2 + 4\frac{Rd\mathrm{e}^{\beta y}}{3RPr}\frac{\partial^2\theta}{\partial y^2} + \frac{M^2Ec}{R}\mathrm{e}^{\beta y}u^2,$$

$$\frac{\partial u}{\partial y} = \alpha\sigma_1\left(u_{B1} - \frac{R}{{\sigma_1}^2}P\right) \quad \text{at } y = 0,$$

$$\frac{\partial u}{\partial y} = -\alpha\sigma_2\left(u_{B2} - \frac{R}{{\sigma_2}^2}P\right) \quad \text{at } y = 1.$$

With the flow being governed by pressure gradient

$$-\frac{\partial p}{\partial x} = \left(\frac{\partial p}{\partial x}\right)_s + \left(\frac{\partial p}{\partial x}\right)_0 \mathrm{e}^{\mathrm{i}\omega t},$$

the velocity and temperature are assumed to be of the form

$$u = u_s + u_0\mathrm{e}^{\mathrm{i}\omega t}, \qquad \theta = T_s + T_0\mathrm{e}^{\mathrm{i}\omega t}.$$

Steady flow equations and boundary conditions:

$$\frac{\mathrm{d}^2u_s}{\mathrm{d}y^2} - (R+\beta)\frac{\mathrm{d}u_s}{\mathrm{d}y} - M^2\mathrm{e}^{\beta y}u_s = RP_s, \tag{5}$$

$$\left(1 + \frac{4Rd}{3}\right)\frac{\mathrm{d}^2T_s}{\mathrm{d}y^2} - R\mathrm{e}^{-\beta y}\frac{\mathrm{d}T_s}{\mathrm{d}y} + Br\mathrm{e}^{-\beta y}\left(\frac{\partial u_s}{\partial y}\right)^2 + M^2Bru_s^2 = 0, \tag{6}$$

$$\frac{\partial u_s}{\partial y} = \alpha\sigma_1\left(u_{sB1} - \frac{R}{\sigma_1^2}P_s\right) \quad \text{at } y = 0, \tag{7}$$

$$\frac{\partial u_s}{\partial y} = -\alpha\sigma_2\left(u_{sB2} - \frac{R}{\sigma_2^2}P_s\right) \quad \text{at } y = 1. \tag{8}$$

The oscillatory flow equations:

$$\frac{\mathrm{d}^2u_0}{\mathrm{d}y^2} - (R+\beta)\frac{\mathrm{d}u_0}{\mathrm{d}y} - \left(R\mathrm{i}\omega + M^2\mathrm{e}^{\beta y}\right)u_0 = RP_0, \tag{9}$$

$$\left(1 + \frac{4Rd}{3}\right)\frac{d^2T_0}{y^2} - RPr\mathrm{e}^{-\beta y}\left(\frac{\mathrm{d}T_0}{\mathrm{d}y} + \mathrm{i}\omega T_0\right) + 2Br\mathrm{e}^{-\beta y}\left(\frac{\partial u_s}{\partial y}\frac{\partial u_0}{\partial y}\right),$$
$$+ 2M^2Bru_su_0 = 0, \tag{10}$$

$$\frac{\partial u_0}{\partial y} = \alpha\sigma_1\left(u_{0B1} - \frac{R}{\sigma_1^2}P_0\right) \quad \text{at } y = 0, \tag{11}$$

$$\frac{\partial u_0}{\partial y} = -\alpha\sigma_2\left(u_{0B2} - \frac{R}{\sigma_2^2}P_0\right) \quad \text{at } y = 1. \tag{12}$$

1.2 Solution of the problem

The pulsatile flow solution is provided by

$$u = u_s + u_0 \mathrm{e}^{\mathrm{i}\omega t}, \qquad \theta = T_s + T_0 \mathrm{e}^{\mathrm{i}\omega t}. \tag{13}$$

To solve the steady and oscillatory flow equations subject to boundary conditions (5)–(13), we employed the shooting method in conjunction with the classical fourth-order Runge–Kutta (RK-4) scheme. The governing higher-order differential equations were systematically reduced to an equivalent system of first-order ordinary differential equations. This transformation enabled the reformulation of the boundary value problem into an initial value problem, where the unknown initial slopes were iteratively refined using Newton's method. Numerical integration was carried out using Mathematica's built-in NDSolve function, facilitating efficient and accurate computation. While numerical solutions can become challenging – particularly in cases where boundary conditions are poorly defined or the governing equations exhibit strong nonlinearity or stiffness – such complications are absent in the current flow model. However, in the present flow situation, boundary conditions are well-posed and physically consistent, and the governing system is non-stiff. These factors collectively contribute to the robustness and accuracy of the adopted numerical approach, enhancing the effectiveness of the NDSolve routine for the present problem.

- *Nusselt number*. The Nusselt number is crucial in heat transfer as it quantifies the enhancement of convective heat transfer relative to pure conduction. It helps assess thermal performance, optimize heat exchanger designs, and analyze the effects of flow conditions, including variable viscosity and density in stratified fluid systems [11].

$$Nu = \left(\frac{\partial \theta}{\partial y}\right)_{y=0,1}$$

- *Entropy generation*. Entropy generation between permeable beds is crucial for optimizing energy efficiency, reducing irreversibilities and improving heat transfer in porous systems. It helps analyze flow stability, pressure losses, and the impact of variable density and viscosity in stratified fluid flows [10, 26].

$$Eg = \left(\frac{\partial T}{\partial y}\right)^2\left(1 + \frac{4Rd}{3}\right) + \frac{1}{\Omega}\left(Br\mathrm{e}^{-\beta y}\left(\frac{\partial u}{\partial y}\right)^2 + BrM^2u^2\right).$$

- *Bejan number*. The Bejan number is important in analyzing the balance between heat transfer irreversibility and fluid friction irreversibility in thermal systems. It helps optimize energy efficiency, minimize entropy generation, and improve the

design of heat exchangers and liquid flow systems, especially in stratified and porous media.

$$Be = \frac{(\frac{\partial T}{\partial y})^2(1 + \frac{4Rd}{3})}{Eg}.$$

- *Mass flux*. The rate of mass flow per unit area in stratified fluid flow between permeable beds is [11, 15]

$$Q = \int_0^1 u \, \mathrm{d}y.$$

- *Shear stress*. It represents the resistive force arising from fluid layer interactions in stratified flow between permeable beds, and it is given by

$$\tau = \mathrm{e}^{-\beta y} \frac{\partial u}{\partial y}.$$

2 Results and discussion

This study explores entropy generation for pulsating stratified fluid flow between permeable beds, incorporating viscous dissipation and radiative heat flux effects for fixing the values $R = 2$, $\beta = 1$, $M = 1$, $P_s = P_0 = 1$, $\sigma_2 = \sigma_1 = 5$, $\alpha = 0.5$, $\omega t = \pi/4$, $Pr = 1$, $Rd = 1$, $Br = 1$, $\Omega = 1$.

Figure 2(a) shows that as the Hartmann number rises, the fluid velocity falls due to the stronger magnetic field generating a resistive Lorentz force that opposes the fluid's motion regardless of the permeable bed. Similarly, Fig. 2(b) indicates that an elevated slip parameter leads to a reduction in velocity, whether the bed is permeable or impermeable, suggesting higher slip conditions result in greater resistance at the fluid interface. Figure 2(c) reveals that an increase in the stratification parameter reduces velocity regardless of permeability, strongly influenced by the applied magnetic field and permeability. In contrast, Fig. 2(d) shows that a rise in pressure gradient enhances the fluid's velocity whether the bed is permeable or impermeable. Furthermore, in Fig. 2(e), the rise in frequency parameter causes a fall in velocity, whether the bed is permeable or impermeable. Figure 2(f) depicts that an increase in the Reynolds number, acting as a suction/injection parameter (0.1 to 2.5), enhances velocity by reducing viscous resistance and increasing inertial effects. However, Fig. 2(g) demonstrates that when the Reynolds number reaches 2.5, the velocity trend reverses in the presence of permeability, while no noticeable change occurs in its absence. Finally, Fig. 2(h) shows that the unsteady velocity component fluctuates over time, reflecting the unsteady nature of the flow. Figure 3 demonstrates that the impact on temperature is observed in both permeable and nonpermeable bed scenarios. As the Brinkman number rises (Fig. 3(a)), temperature increases due to enhanced viscous dissipation. In contrast, a higher Prandtl number (Fig. 3(b)) leads to a temperature drop as reduced heat conduction lowers the temperature gradient. Similarly, increasing the Hartmann number (Fig. 3(c)) temperature decreases because magnetic field resistance

limits convective heat transfer. On the other hand, greater radiative heat flux (Fig. 3(d)) raises the temperature by absorbing more radiant energy. A rise in the pressure gradient (Fig. 3(e)) also results in higher temperatures. However, as the Reynolds number increases (Fig. 3(f)), temperature decreases owing to reduced viscous heating. Additionally, a higher stratification parameter (Fig. 3(g)) causes a temperature rise, while Fig. 3(h) depicts fluctuations in the unsteady temperature component over time.

Figure 4(a) shows that with the increasing stratification parameter, the Nusselt number decreases at the lower bed due to reduced convective heat transfer, as stratification suppresses vertical mixing and thermal transport. However, at the upper bed, the Nusselt number increases because the enhanced thermal stability and reduced mixing promote more efficient heat transfer. Figures 4(b), 4(c), and 4(d) demonstrate that as the Hartmann number, Prandtl number, and permeability parameter rise, the Nusselt number decreases at the lower permeable bed. This is due to the increased resistance to flow from the magnetic field, enhanced thermal diffusivity, and permeability, which limit convective heat transfer. Conversely, at the upper permeable bed, a reverse trend is observed, indicating that these parameters enhance convective heat transfer and thermal stability, improving heat transport efficiency in that region. This reflects the complex interplay between fluid dynamics, thermal properties, and permeability variations within the stratified medium.

The impact on entropy generation is observed in both permeable and nonpermeable bed conditions, as shown in Figs. 5, 6. Figure 5(a) shows that as the Brinkman number increases, entropy generation rises due to greater viscous dissipation, while the Bejan number falls, indicating a higher proportion of irreversibility in heat transfer relative to fluid flow. Figure 5(b) demonstrates that an increase in the stratification parameter raises entropy generation near the lower bed due to reduced convective heat transfer, while near the upper bed, it decreases as stratification enhances thermal stability, and the Bejan number increases, indicating improved efficiency in heat transfer. Figures 5(c) and 5(d) reveal that higher Prandtl and permeability parameters reduce entropy generation near the lower bed by promoting better heat conduction and flow stability but show the opposite trend near the upper bed, where increased permeability enhances convective heat transfer. The Bejan number is inversely related to entropy generation, reflecting a shift in the balance between thermal and flow irreversibilities. Figure 6 indicates that for the Hartmann number, entropy generation decreases near both the lower and upper beds due to the magnetic field's suppression of convective heat transfer, but increases in the middle zone due to enhanced viscous dissipation with the Bejan number following the reverse trend.

Figures 7(a) and 7(c) show that as the Reynolds number and pressure gradient rise, mass flux grows in both porous and nonporous cases. A higher Reynolds number indicates that inertial forces dominate over viscous forces, enhancing bulk fluid movement and mass transport, while an increased pressure gradient serves as a driving force that pushes the fluid more effectively in the region. However, in Figs. 7(b) and 7(d), regardless of permeability, the opposite behavior is observed with the stratified fluid parameter and Hartmann number. The increase in the stratified fluid parameter enhances fluid density stratification, which suppresses vertical mixing and reduces mass flux. Similarly, a higher Hartmann number intensifies the Lorentz force, which acts as a resistive damping force on the fluid motion, thereby decreasing the overall mass transport within the channel.

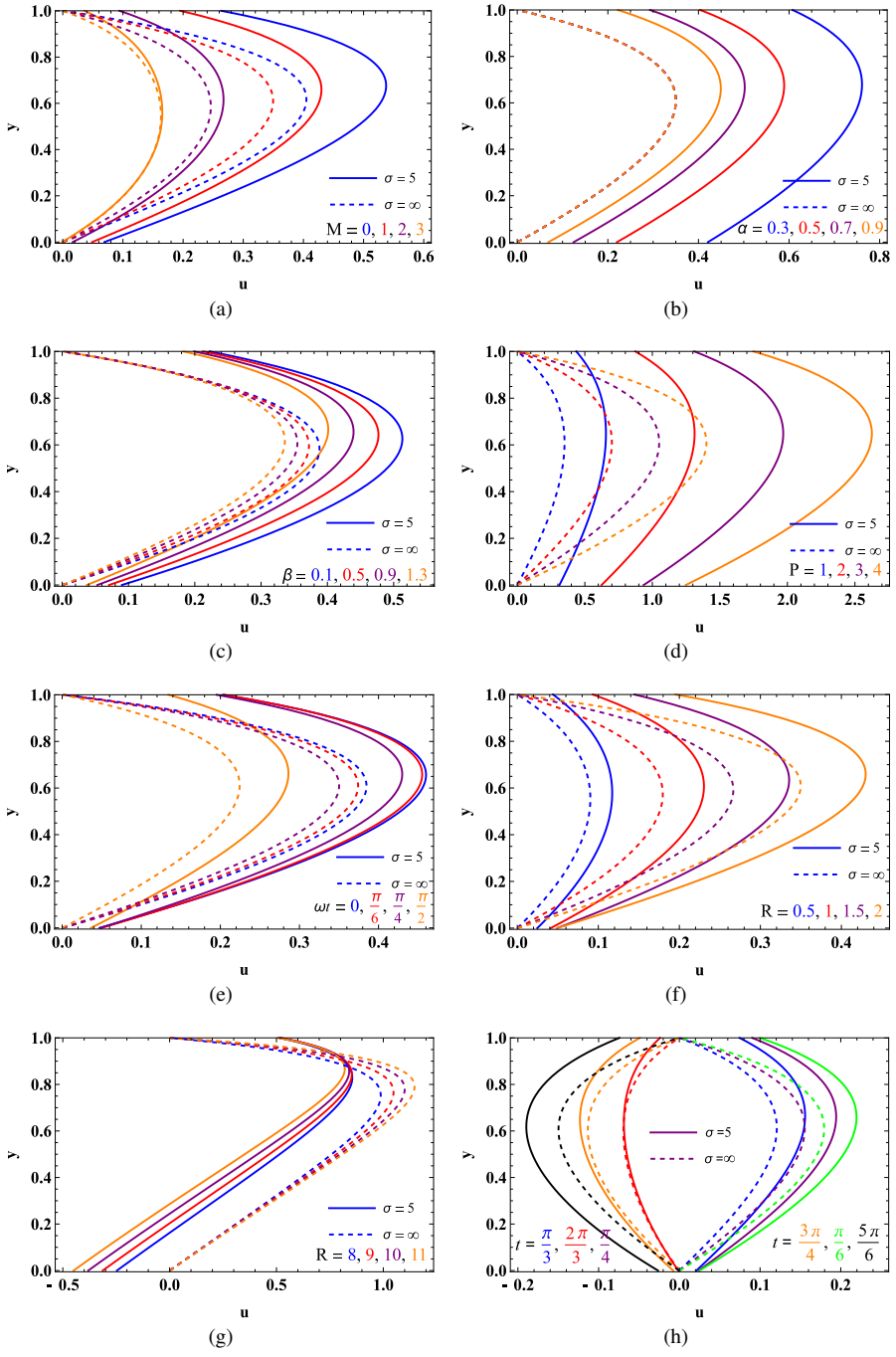

Figure 2. Velocity variation with different parameters.

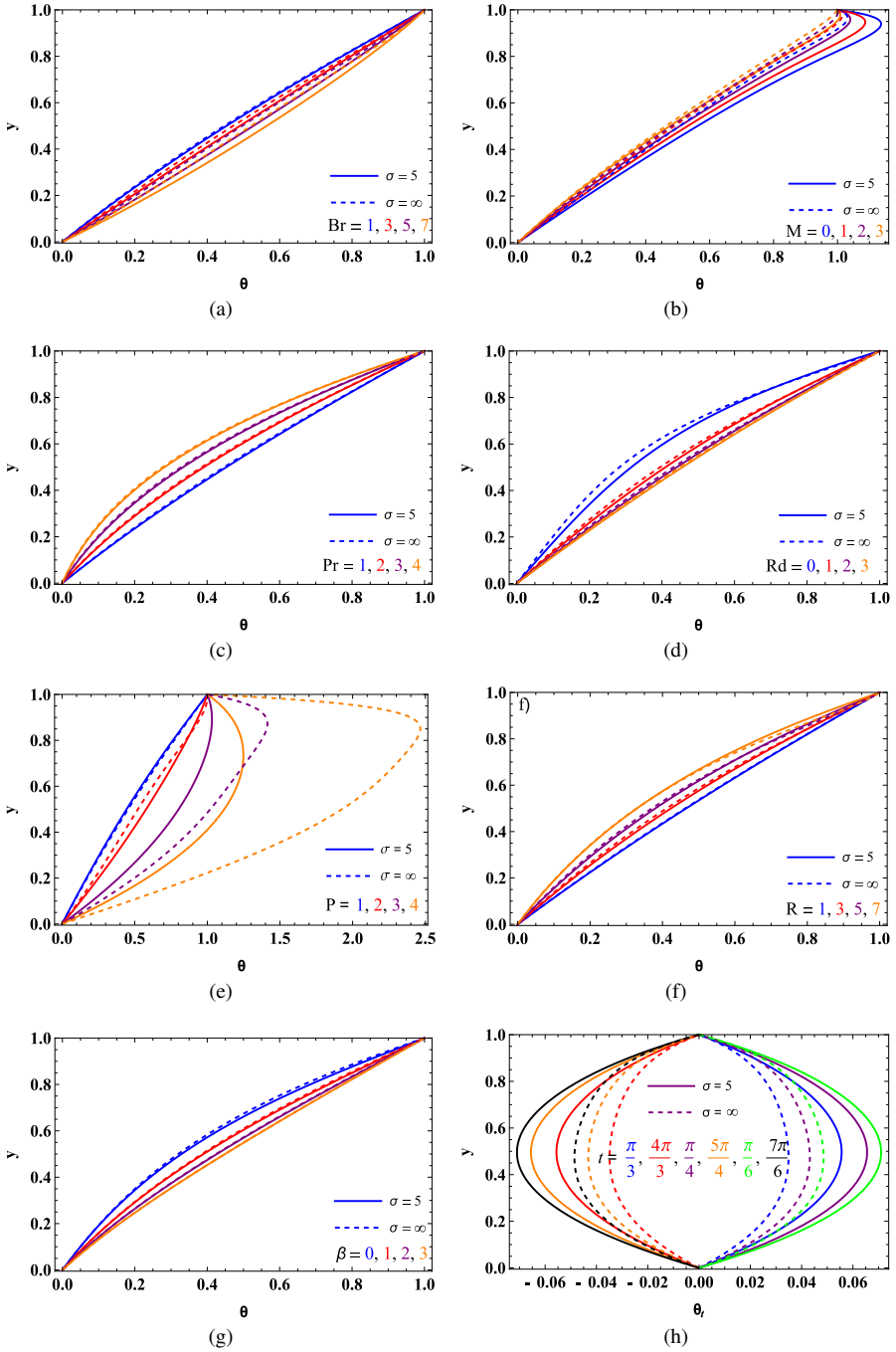

Figure 3. Temperature variation with different parameters.

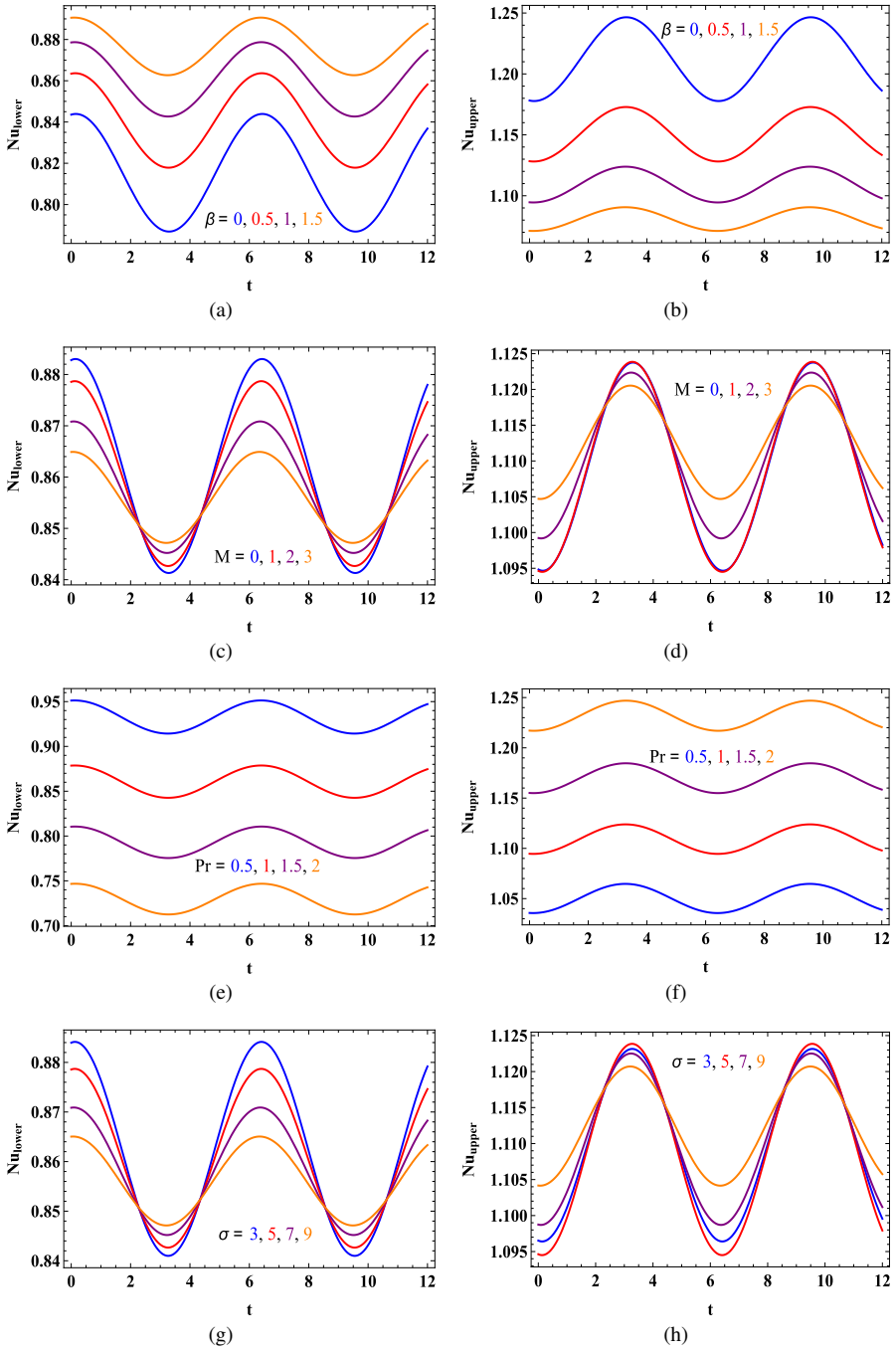

Figure 4. Nusselt number variation with different parameters.

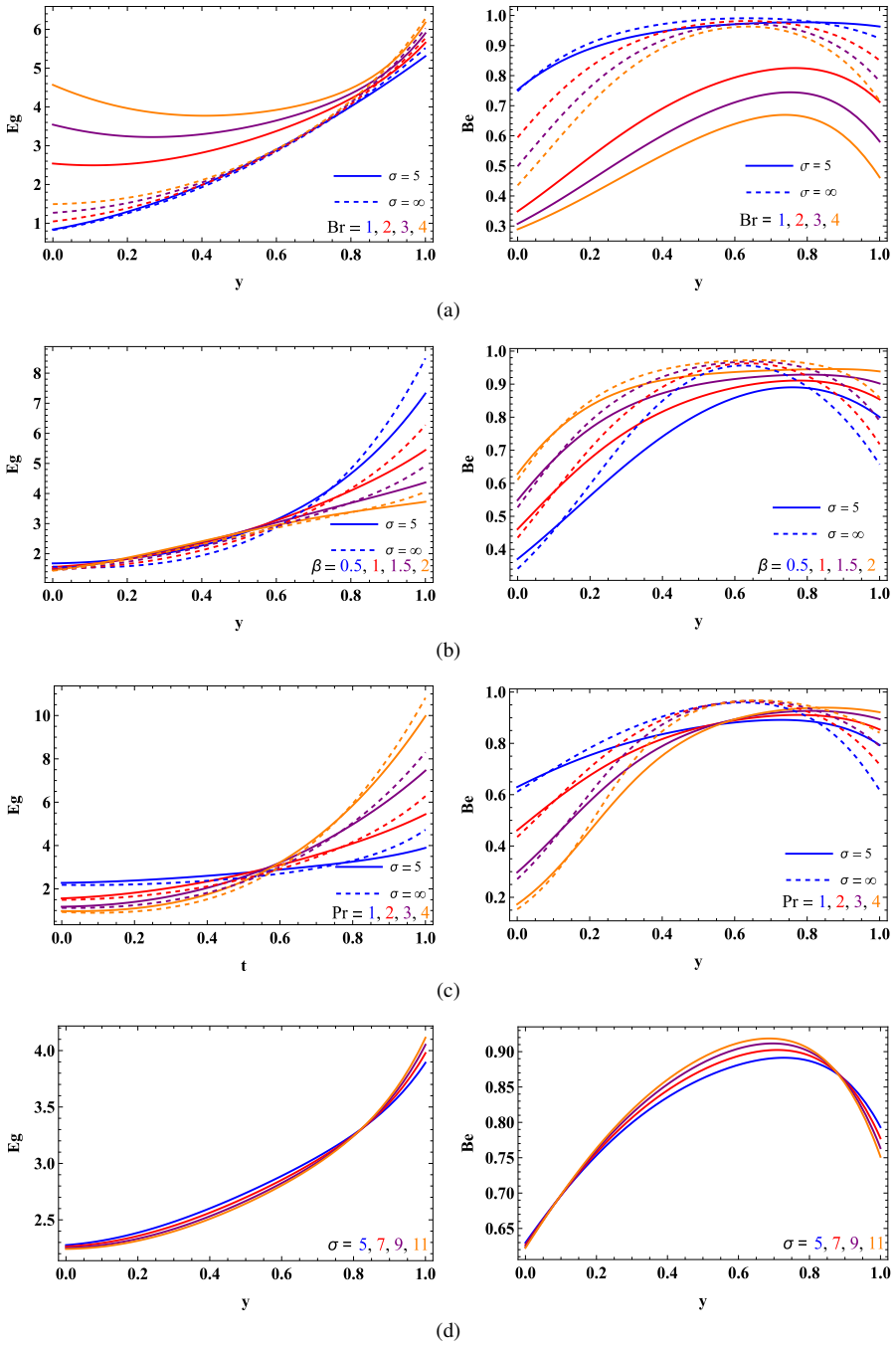

Figure 5. Entropy generation and Bejan number variation with various parameters.

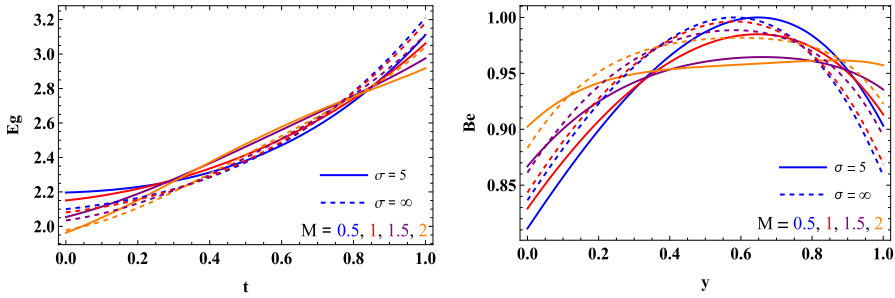

Figure 6. Entropy generation and Bejan number variation with various parameters.

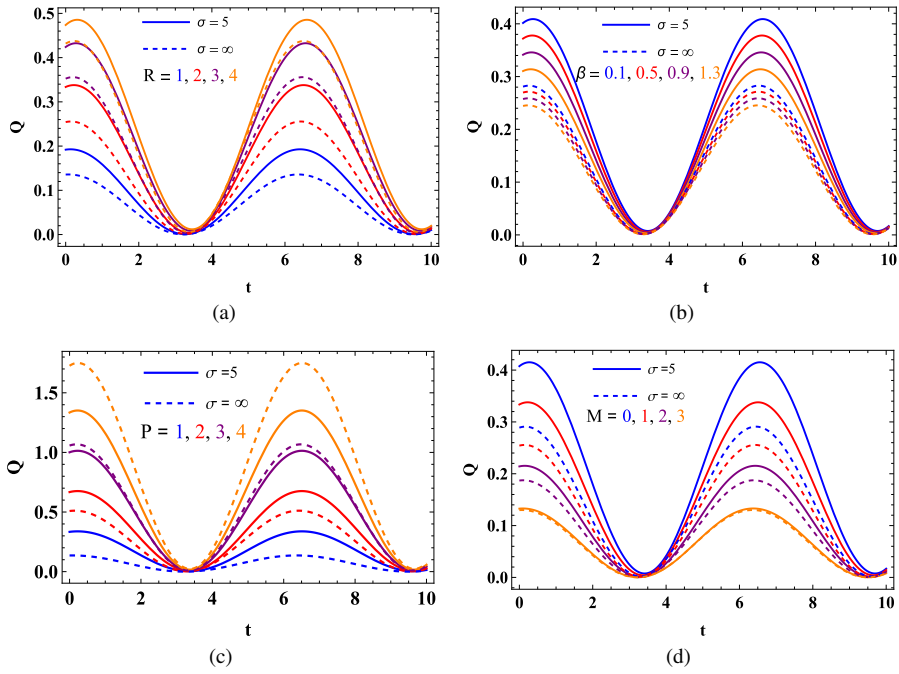

Figure 7. Mass flux variation with different parameters.

As the Hartmann number rises, shear stress decreases at both permeable boundaries (Fig. 8(a)) due to the magnetic field opposing the liquid motion and reducing the velocity gradient. Figure 8(b) shows that with a rise in the stratified liquid parameter, shear stress decreases at both the UPB and LPB, likely due to enhanced thermal stability and reduced fluid mixing. Figure 8(c) demonstrates that with a rise in the permeability parameter, shear stress decreases at the LPB, where enhanced permeability reduces flow resistance, while shear stress increases at the UPB, where higher permeability promotes greater fluid movement and shear at the interface.

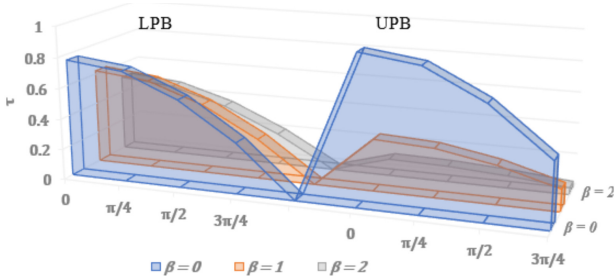

(a)

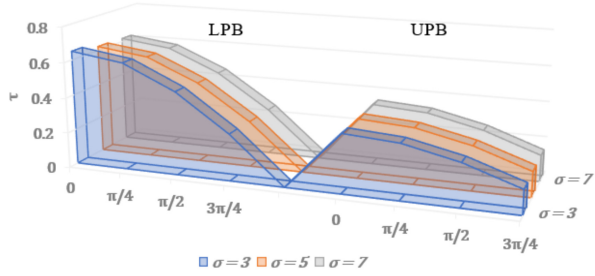

(b)

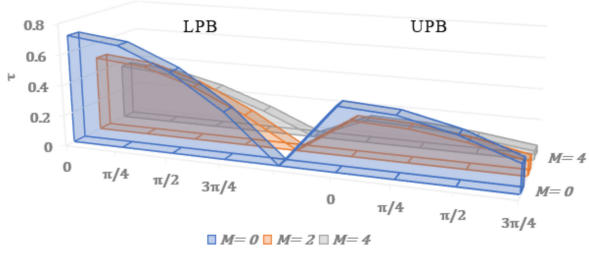

(c)

Figure 8. Shear stress variation with pertinent parameters.

Figure 9 presents a comparison, revealing excellent agreement with the findings of [15] for $\beta = 0$ and [2] for $M = 0$.

Our analysis demonstrates that stratification strongly affects both velocity and temperature distributions. It promotes velocity reduction under a magnetic field, whereas temperature growth is influenced by the Brinkman number, i.e., as the stratification parameter rises from 0 to 1, the percentage reduction in velocity is 14.6 at $M = 0$, and it raises to 18.5 when Hartmann number reaches to 1, while for the nonporous case, the velocity reduces to 8.6% and 10.7%, respectively. Similarly, as the stratification parameter rises from 0 to 1, the percentage rise in temperature distribution is 17.2 at $Br = 0$, and it is diminished to 2.9 when the Brinkman number equals to 1 ($Br = 1$), whereas for no permeability (walls are rigid), the temperature rises to 15.2% and 2.5%, respectively.

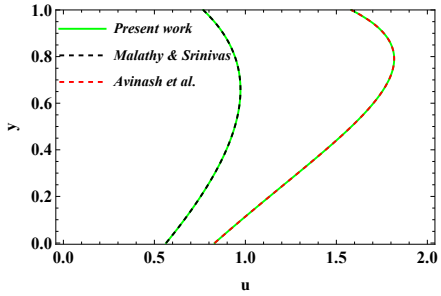

Figure 9. Comparative analysis.

3 Conclusions

This investigation focuses on entropy generation for magnetohydrodynamic (MHD) pulsating stratified liquid flow between permeable beds. The fluid flow system involves equal-velocity injection through the lower bed and extraction through the upper bed. The governing equations are solved employing the fourth-order Runge–Kutta method coupled with the shooting method in Mathematica. The impact of key parameters on flow variables has been presented and discussed. Key observations are:

- An increase in the Hartmann number, along with the slip, stratification, and frequency parameters, leads to a significant reduction in velocity, regardless of whether the bed is permeable or not. Moreover, in the presence of a permeable bed and high suction/injection (Reynolds number), the velocity decreases, and it shows the opposite trend when there is no permeability. However, in the absence of permeability, the velocity shows an increasing trend at low Reynolds numbers (suction/injection parameter). Additionally, the pressure gradient induces an increase in velocity.
- The temperature is elevated by rising Brinkman number, radiative heat flux, and stratified fluid parameter, whereas it is diminished by rising Hartmann number, Prandtl number, pressure gradient, and Reynolds number, regardless of whether the bed is permeable or not.
- Unsteady velocity, temperature distributions oscillate over time regardless of the permeability of the bed.
- As the Brinkman number rises, entropy generation enhances, while the Bejan number drops, regardless of the permeability of the bed.
- An elevated stratified parameter raises entropy generation near the lower bed but reduces it near the upper bed, where the Bejan number rises whether the bed is permeable or impermeable.
- Higher Prandtl and permeability parameters reduce entropy generation near the lower bed but show the opposite trend near the upper bed.
- For the Hartmann number, entropy generation decreases near the lower and upper beds but increases in the middle zone, with the Bejan number following the reverse trend, whether the bed is permeable or impermeable.

- The rate of heat transfer falls with the stratified fluid parameter, Hartmann number, Prandtl number, and permeability parameters at the lower bed (Nulower) but exhibits the opposite trend at the upper bed, regardless of the permeability of the bed.
- As the Reynolds number and pressure gradient increase, mass flux rises; however, it exhibits the opposite behavior with the stratified fluid parameter and Hartmann number whether the bed is permeable or impermeable.
- With the rise of stratified parameter and Hartmann number, shear stress falls at both the UPB and LPB. However, with a rise in the permeability parameter, shear stress reduces at LPB but rises at UPB.
- A comparative analysis has been conducted with the previous works of [15], as well as [2], showing good agreement with our results and validating their accuracy.

Hopefully, this study will aid in assessing the accuracy of numerical solutions for more complex problems in this domain, particularly those involving a greater number of physical parameters. While various studies have been conducted on pulsatile flow, to the best of the authors' knowledge, no analytical or numerical work has been reported on the thermal aspects of stratified fluid flow between permeable beds. The heat transfer characteristics of pulsating stratified flow incorporating rheological effects between permeable beds remain an open problem from the authors' perspective. Furthermore, investigation related to the thermal behavior of starting flow (induced by a sudden pressure gradient) has not yet been explored to the best of the authors' knowledge.

Conflicts of interest. The authors declare no conflicts of interest.

Appendix

Table 1. Nomenclature.

Symbol	Description	Unit (SI)
u	Velocity	$\mathrm{m/s}$
t	Time	s
T	Temperature	K
h	Channel height	m
V	Suction/injection parameter	–
ρ	Density	$\mathrm{kg/m^3}$
μ	Dynamic viscosity	Pa s
σ	Electrical conductivity	$\mathrm{S/m}$
Ω	Dimensionless temperature difference	–
α	Slip parameter	–
P	Pressure	Pa
β	Stratification parameter	–
M	Hartmann number	–
R	Reynolds number	–
Pr	Prandtl number	–
ΔT	Temperature difference	K
C_p	Specific heat	$\mathrm{J/(kgK)}$

Continued on next page

Table 1 (*contined from previous page*)

Symbol	Description	Unit (SI)
B_0	External magnetic field	T
Rd	Radiation parameter	–
Br	Brinkman number	–
Nu	Nusselt number	–
Be	Bejan number	–
Eg	Entropy generation	$\mathrm{W}/(\mathrm{m}^3\mathrm{K})$
Q_1, Q_2	Velocities inside the porous beds	m/s
σ_1, σ_2	Dimensionless permeability parameters	–
u_{B1}, u_{B2}	Velocities at lower/upper permeable beds	m/s
u_s, u_0	Steady and oscillatory velocity components	m/s
T_s, T_0	Steady and oscillatory temperature components	K
x, y	Cartesian coordinates	m

References

1. A.M. Ardekani, R. Stocker, Stratlets: Low reynolds number point-force solutions in a stratified fluid, *Phys. Rev. Lett.*, **105**(8):084502, 2010, https://doi.org/10.1103/PhysRevLett.105.084502.
2. K. Avinash, J. Anand Rao, S. Sreenadh, Y.V.K. Ravi Kumar Kumar, Pulsatile flow of a viscous stratified fluid of variable viscosity between permeable beds, *J. Porous Media*, **14**(12):1115–1124, 2011, https://doi.org/10.1615/JPorMedia.v14.i12.60.
3. G.S. Beavers, D.D. Joseph, Boundary conditions at a naturally permeable wall, *J. Fluid Mech.*, **30**(1):197–207, 1967, https://doi.org/10.1017/S0022112067001375.
4. M.N. Channabasappa, G. Ranganna, Flow of viscous stratified fluid of variable viscosity past a porous bed, *Proc. Indian Acad. Sci., Sect. A*, **83**(4):145–155, 1976, https://doi.org/10.1007/BF03051375.
5. R. Choudhari, D. Tripathi, H. Vaidya, K.V. Prasad, J. Shetty, F. Mebarek-Oudina, S.U. Khan, K. Ramesh, Integrated analysis of electroosmotic and magnetohydrodynamic peristaltic pumping in physiological systems: Implications for biomedical applications, *ZAMM, Z. Angew. Math. Mech.*, **104**(8):e202400163, 2024, https://doi.org/10.1002/zamm.202400163.
6. H. Darcy, *Les Fontaines Publiques de la Ville de Dijon*, Victor Dalmont, Paris, 1856.
7. M.P. Devi, S. Srinivas, Heat transfer effects on the oscillatory MHD flow in a porous channel with two immiscible fluids, *Nonlinear Anal. Model. Control*, **28**(3):393–411, 2023, https://doi.org/10.15388/namc.2023.28.31503.
8. K. Goyal, S. Srinivas, Two-layered magnetohydrodynamics of immiscible pulsatile flow in corrugated curved channel, *Int. J. Model. Simul.*, **45**(6):1993–2011, 2025, https://doi.org/10.1080/02286203.2024.2311967.
9. J. Josuva, R.H. Reddy, Pulsatile hydromagnetic Carreau–Yasuda nanofluid flow in a nonlinearly radiated inclined porous channel with nonuniform heat source/sink: Entropy analysis, *ZAMM, Z. Angew. Math. Mech.*, **105**(5):e70092, 2025, https://doi.org/10.1002/zamm.70092.
10. K.R. Kavitha, C.V.R. Murthy, MHD influence on second order fluid flow over an inclined permeable bed, *AIP Conf. Proc.*, **2707**(1), 2023, https://doi.org/10.1063/5.0143092.

11. D. Kumar, M. Agarwal, MHD pulsatile flow and heat transfer of two immiscible couple stress fluids between permeable beds, *Kyungpook Math. J.*, **61**(2):323–351, 2021, https://doi.org/10.5666/KMJ.2021.61.2.323.
12. P.B. Kumar, S. Srinivas, Pulsating flow of a non-newtonian nanofluid in a porous channel with magnetic field, *Mater. Today Proc.*, **9**:320–332, 2019, https://doi.org/10.1016/j.matpr.2019.02.162.
13. R.R. Long, Some aspects of the flow of stratified fluids: I. A theoretical investigation, *Tellus*, **5**(1):42–58, 1953, https://doi.org/10.3402/tellusa.v5i1.8563.
14. Vangalapudi M., S. Srinivas, Flow of couple-stress and micropolar immiscible liquid layers between permeable beds with entropy generation, *J. Heat Mass Transf. Res.*, **13**(1), 2026, https://doi.org/10.22075/jhmtr.2025.37292.1707.
15. T. Malathy, S. Srinivas, Pulsating flow of a hydromagnetic fluid between permeable beds, *Int. Commun. Heat Mass Transfer*, **35**(5):681–688, 2008, https://doi.org/10.1016/j.icheatmasstransfer.2007.12.006.
16. P.K. Mandal, An unsteady analysis of nonlinear two-layered 2D model of pulsatile flow through stenosed arteries, *Math. Model. Anal.*, **8**(3):229–246, 2003, https://doi.org/10.1080/13926292.2003.9637226.
17. S. Mukherjee, G.C. Shit, Mathematical modeling of electrothermal couple stress nanofluid flow and entropy in a porous microchannel under injection process, *Appl. Math. Comput.*, **426**:127110, 2022, https://doi.org/10.1016/j.amc.2022.127110.
18. M. Muzammal, M. Farooq, Hashim, H. Alotaibi, Transportation of melting heat in stratified Jeffrey fluid flow with heat generation and magnetic field, *Case Stud. Therm. Eng.*, **58**:104465, 2024, https://doi.org/10.1016/j.csite.2024.104465.
19. D.A. Nield, The beavers–joseph boundary condition and related matters: A historical and critical note, *Transp. Porous Media*, **78**:537–540, 2009, https://doi.org/10.1007/s11242-009-9344-y.
20. M. Padma Devi, S. Srinivas, K. Vajravelu, Entropy generation in two-immiscible MHD flow of pulsating Casson fluid in a vertical porous space with slip effects, *J. Therm. Anal. Calorim.*, **149**(14):7449–7468, 2024, https://doi.org/10.1007/s10973-024-13337-8.
21. K.J. Pillai, S.V.K. Varma, M.S. Babu, Aligned magnetic effects through varying permeable bed, *Proc. Indian Acad. Sci., Math. Sci.*, **96**:61–69, 1987, https://doi.org/10.1007/BF02837796.
22. O. Prakash, D. Kumar, Y.K. Dwivedi, Heat transfer in MHD flow of dusty viscoelastic (Walters' liquid model-B) stratified fluid in porous medium under variable viscosity, *Pramana*, **79**(6):1457–1470, 2012, https://doi.org/10.1007/s12043-012-0344-z.
23. X. Qu, D. Fang, X. Qi, Direct contact heat transfer enhancement between two stratified immiscible fluids by artificial interface oscillations, *Int. J. Heat Mass Transfer*, **138**:226–234, 2019, https://doi.org/10.1016/j.ijheatmasstransfer.2019.04.064.
24. G. Radhakrishnamacharya, M.K. Maiti, Heat transfer to pulsatile flow in a porous channel, *Int. J. Heat Mass Transfer*, **20**(2):171–173, 1977, https://doi.org/10.1016/0017-9310(77)90009-6.
25. J. Raza, F. Mebarek-Oudina, H. Ali, I.E. Sarris, Slip effects on casson nanofluid over a stretching sheet with activation energy: RSM analysis, *Front. Heat Mass Transfer*, **22**(4):1017–1041, 2024, https://doi.org/10.32604/fhmt.2024.052749.

26. J. Srinivas, J.V. Ramana Murthy, K.S. Sai, Entropy generation analysis of the flow of two immiscible couple stress fluids between two porous beds, *Comput. Therm. Sci., Int. J.*, **7**(2), 2015, https://doi.org/10.1615/ComputThermalScien.2015012175.

27. J. Srinivas, J.V. Ramana Murthy, Flow of two immiscible couple stress fluids between two permeable beds, *J. Appl. Fluid Mech.*, **9**(1):501–507, 2015, https://doi.org/10.18869/acadpub.jafm.68.224.24013.

28. S. Srinivas, J.B. Anasuya, V. Merugu, Interaction of pulsatile and peristaltic flow of a particle-fluid suspension with thermal effects, *Int. Commun. Heat Mass Transfer*, **163**:108728, 2025, https://doi.org/10.1016/j.icheatmasstransfer.2025.108728.

29. X.-H. Tan, X.-J. Zhou, P. Xu, Y. Zhu, D.-J. Zhuang, A fractal geometry-based model for stress-sensitive permeability in porous media with fluid-solid coupling, *Powder Technol.*, **455**:120774, 2025, https://doi.org/10.1016/j.powtec.2025.120774.

30. H. Vaidya, K.V. Prasad, M.I. Khan, F. Mebarek-Oudina, I. Tlili, C. Rajashekhar, S. Elattar, M.I. Khan, S.G. Al-Gamdi, Combined effects of chemical reaction and variable thermal conductivity on MHD peristaltic flow of Phan-Thien-Tanner liquid through inclined channel, *Case Stud. Therm. Eng.*, **36**:102214, 2022, https://doi.org/10.1016/j.csite.2022.102214.

31. K. Vajravelu, K. Ramesh, S. Sreenadh, P.V. Arunachalam, Pulsatile flow between permeable beds, *Int. J. Non-Linear Mech.*, **38**(7):999–1005, 2003, https://doi.org/10.1016/S0020-7462(02)00045-8.

32. Y. Yang, Q. Zhang, General properties of a multilayer stratified fluids system, *Phys. Fluids, A*, **5**(5):1167–1181, 1993, https://doi.org/10.1063/1.858602.

33. J. Yao, K. Tao, Z. Huang, Flow of particulate-fluid suspension in a channel with porous walls, *Transp. Porous Media*, **98**:147–172, 2013, https://doi.org/10.1007/s11242-013-0137-y.